IR Spectroscopic Study of the Structure and Phase Behavior of Long-Chain Diacylphosphatidylcholines in the Gel State

R. G. Snyder,* G. L. Liang,* H. L. Strauss,* and R. Mendelsohn#
*Department of Chemistry, University of California, Berkeley, Berkeley, California 94720-1460 and #Department of Chemistry, Newark College of Arts and Science, Rutgers University, Newark, New Jersey 07102 USA

ABSTRACT Fully hydrated dispersions of simple linear saturated diacylphosphatidylcholines with even-numbered acyl chains of lengths from 18 to 24 carbons can exist in a low-temperature, highly ordered, orthorhombic phase (G_o) that differs from the $L_{\beta'}$ phase (G_d) normally found for shorter chains. The temperature behavior of these dispersions has been studied by infrared spectroscopy. Chain packing in the G_o phase was found to be nearly identical to that of the orthorhombic phase of crystalline *n*-alkanes. With increasing temperature, the G_o phase undergoes a transition to G_d at ~45°C below T_m. This transition occurs at a higher temperature and becomes sharper with increasing chain length. Chain packing in the G_d phase was found to be disordered in a way that can be expressed in terms of a distribution of subcell setting angles. The G_d phase converts to a phase (G_h) with hexagonal-like chain packing at temperatures below T_m. The results support and extend those of a recent x-ray diffraction study of the 24-carbon diacylphosphatidylcholine gel.

INTRODUCTION

We explore by infrared (IR) spectroscopy the unique phase behavior of "long-chain," simple linear saturated diacylphosphatidylcholine (PC) bilayers in fully hydrated gel-state dispersions. By "long-chain" PCs we refer to even-numbered acyl chains with lengths from 18 to 24 carbons, to be distinguished from "short-chain" PCs with lengths from 12 to 16 carbons.

Sun et al. (1996) recently reported that long-chain PCs in the gel state exhibit phase behavior markedly different from that of the much studied short-chain PCs (Cevc and Marsh, 1987; Lewis and McElhaney, 1991). They demonstrated from x-ray diffraction measurements that gel-state $diC_{24}PC$ at room temperature can exist in an orthorhombic phase that is more densely packed than the usual gel phase, commonly referred to as the $L_{\beta'}$ phase. On warming, this phase converts to $L_{\beta'}$. Further warming results in a second transition to a phase in which the chain packing is apparently hexagonal.

We report here an IR study on the chain packing and phase behavior of a series of long-chain PCs, diC_nPC (n_{even} = 18–24), over the temperature range from −20°C to T_m, the main (gel-to-liquid-crystal) transition temperature. Where our results overlap those from the diffraction study (Sun et al., 1996), which focuses mainly on $diC_{24}PC$, there is general agreement.

The anomalous phase behavior of long-chain PCs was touched on in an earlier IR study of microaggregation in gel-state binary mixtures (Mendelsohn et al., 1995). In IR studies related to the present research, Cameron and coworkers (1980 and 1981) reported on the ripple phase of $diC_{16}PC$ and on acyl-chain packing in bilayers of a variety of phospholipids with different chain lengths and headgroups.

Various designations have been used to distinguish the gel-state phases of the phospholipids. The ones used by us and by Sun et al. (1996) are listed in Table 1, along with a set frequently used in the literature (Lewis and McElhaney, 1991). A brief description of the packing geometry that characterizes each phase is included.

The short-chain gel-state dispersions are known to exist in at least three phases: the subgel phase (G_s), the usual orthorhombic phase (G_d), and the ripple phase (G_r). A new high-density orthorhombic phase (G_o) was identified for $diC_{24}PC$ by Sun et al. (1996), who also reported a possible second new phase (G_h), a high-temperature form that displays hexagonal-like chain packing, which may or may not be the ripple phase.

In what follows, we describe techniques and methods and then discuss the phases and phase transitions in the approximate order in which they appear as the gel is warmed.

MATERIALS AND METHODS

Experimental procedures

Materials

The phospholipids used were obtained from Avanti Polar Lipids (Alabaster, AL). They are dipalmitoyl-phosphatidylcholine ($diC_{16}PC$), distearoylphosphatidylcholine ($diC_{18}PC$), diarachidoyl-phosphatidylcholine ($diC_{20}PC$), dibehenoylphosphatidylcholine ($diC_{22}PC$), and dilignoceroyl-phosphatidylcholine ($diC_{24}PC$). The samples were used as received. The IR spectra and the differential scanning calorimetry (DSC) determined transition widths of their dispersions were consistent with the high purity (>99%) quoted by the supplier.

Sample preparation

We prepared aqueous dispersions by dissolving a known weight of lipid in $CHCl_3$/MeOH (4:1 or 9:1, v/v). The solvent was removed under a gentle

Received for publication 21 November 1995 and in final form 3 September 1996.

Address reprint requests to Dr. R. G. Snyder, Department of Chemistry, University of California, Berkeley, Berkeley, CA 94720-1460. Tel: 510-642-8531; Fax: 510-643-2156; E-mail: rgs@uclink2.berkeley.edu.

0006-3495/96/12/3186/13 $2.00

TABLE 1 Phospholipid gel-state phases

Phase	Designation			Structure*		
	This paper	Sun et al.#	Lit.§	Packing	Tilt angle¶	Setting angle¶
Subgel	G_s	–	$L_{c'}$	Tri	Small	~0
Ordered orth	G_o	G2	L_β	Orth	0	~47
Usual orth	G_d	G1	$L_{\beta'}$	Orth	~32	~41‖
Ripple	G_r	–	$P_{\beta'}$	Hex	~32	Random**
Hexagonal##	G_h	G3		Hex	~0	Variable

*The chains are all-*trans*.
#Sun et al. (1996).
§Lewis and McElhaney (1991).
¶In degrees.
‖Average.
**Increasingly random with temperature.
##Hexagonal chain packing.

stream of N_2 gas. We ensured complete drying by placing the sample under vacuum (<1 Torr) for ≥2 h. The sample was then hydrated by addition of the appropriate amount of highly purified H_2O to attain a water:lipid weight ratio of ~2:1 and then sealed. Complete dispersal was achieved by vigorous, repetitive, vortex action (induced by use of a touch-activated mixer), with the sample at a temperature above T_m. Complete hydration was verified by the agreement between T_m determined by IR and DSC and the values reported in the literature (Cevc and Marsh, 1987).

The n = 20, 22, 24 dispersions cooled to near −20°C were consistently found to be in the G_o phase. However, this was not the case for n = 18, which was usually G_d, although the addition of 5% of $diC_{20}PC$ seemed to promote G_o. The temperature behavior of the latter "contaminated" mixture was otherwise indistinguishable from that of pure $diC_{18}PC$.

Infrared measurements

We prepared samples for IR measurements by sandwiching the aqueous dispersions between CaF_2 windows separated by a Teflon spacer of thickness 6 μM. The sandwich was fixed in a brass block, which was in turn placed in a thermostated chamber. Temperatures were controlled to 0.1°C with a Neslab refrigerated circulation bath (water or methanol). The lowest temperature attainable with this arrangement was ~−20°C.

The IR spectra were measured with a Nicolet Magna 550 interferometer equipped with a cooled MCT/InSb detector. The spectra were derived from 128 interferograms collected at 1-cm^{-1} resolution, coadded, Fourier transformed with one level of zero filling, and ratioed against a background interferogram. Highly precise band frequencies were determined from second-derivative spectra.

Before their IR spectra were measured, the dispersions were heated above T_m and then slowly cooled to near −20°C over a 1–5-h period. The spectrum was taken first at −19°C and then incrementally as the temperature was increased. The time between measurements was 5–10 min.

We estimated the intensity ratio I_a/I_b (discussed below) by curve-fitting each component band with Voigt-type bands. The spectral background, which consists primarily of methyl bands, was largely eliminated by subtraction of the spectrum of $diC_{18}PC\text{-}d_{70}$ (deuterated acyl chains), measured under the same conditions. We constrained the fitting by fixing the peak frequencies at values determined from second-derivative spectra. The fit to the observed spectrum was improved by introducion of a third band between the two components, which, however, did not appear justified, because it is likely that what we call the "third" band is an artifact that results from asymmetry in the shapes of the component bands.

Calorimetry

DSC measurements were made with a Hart Scientific 707 series calorimeter on samples taken from the same preparations used for the IR measurements. Weighed amounts of the dispersions, sealed tightly in the ampules to avoid loss of water, were first cooled in the calorimeter from room temperature to −30°C over a period of 3 h and then heated from −30 to 90°C at 25°/h during recording. The samples were then recooled to −30°C and the heating step repeated. The two DSC curves were generally the same. We estimated the enthalpy associated with the G_o-to-G_d phase transition by using the observed ratio of the enthalpies for the main transition to that for the G_o-to-G_d transition. The enthalpy of the main transition is available from previous measurements (Lewis et al., 1987; J. Nagle, personal communication).

Infrared band parameters used to monitor chain packing and conformation

The spectral parameters used are associated with methylene wagging (W), antisymmetric C—H stretching (d^-), symmetric C—H stretching (d^+), and scissoring (δ) IR bands. These are identified in Fig. 1, and the motions underlying them are also indicated in terms of a single uncoupled methylene group. The actual normal modes are, however, delocalized, involving essentially all the acyl-chain methylenes in a concerted motion. The relevant properties of these bands will now be briefly discussed.

Methylene wagging bands

The intensities of the wagging bands are dependent on chain packing so that phase transitions are manifest as inflections in intensity-versus- temperature plots. These bands appear between 1170 and 1380 cm^{-1} (Fig. 1) as a progression (Snyder and Schachtschneider, 1963; Snyder, 1967). As temperature increases, the intensities of the bands decrease monotonically, going to zero at T_m (Cameron et al., 1980; Senak et al., 1992).

Earlier studies of crystalline n-alkanes (Snyder et al., 1986) suggest that the temperature dependence of the intensity is closely correlated to the lateral expansion. As the temperature of an n-alkane is increased from 7 K to the melting point the intensities diminish monotonically, with steps at each phase transition. For methylene rocking bands we derived a relation between the temperature coefficients of intensity and lateral expansion. This relation accurately predicts the intensity loss at a phase transition from the change in lateral area (Snyder et al., 1986).

The wagging-band intensities for the PC gel appear to vanish at T_m, whereas those for the other methylene bands do not. (It is not clear whether there is a real difference between the n-alkanes and the PC gels in this respect because the temperature behavior of the n-alkane wagging bands has not been measured.) The uniqueness of the temperature behavior of the wagging intensities for the PC gels is probably related to the fact that the gels' intensities originate in the polar headgroup rather than in the methylene groups themselves.

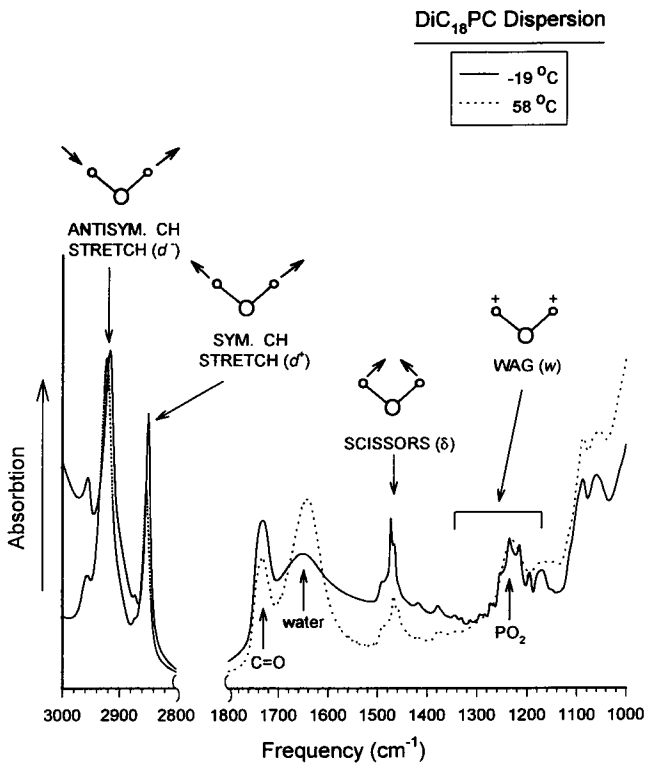

FIGURE 1 IR bands used to monitor the phase behavior of the long-chain phospholipids. These bands, which are marked on the spectrum, represent methylene antisymmetric (d^-) and symmetric (d^+) C—H stretching, scissoring (δ), and wagging (W) modes. The spectra shown are of fully hydrated $diC_{18}PC$ in the gel phase at −19°C (*solid curves*) and in the liquid-crystalline phase at 58°C (*dotted cuves*). The types of methylene hydrogen motion associated with the bands of interest are depicted.

Methylene C—H stretching bands

Polymethylene C—H stretching frequencies increase with increasing conformational disorder (Snyder et al., 1982) and for this reason have been used to estimate lipid bilayer conformational disorder (Moore and Mendelsohn, 1994). The frequencies of the antisymmetric (d^-) and symmetric (d^+) bands for ordered chains near room temperature are near 2920 and 2850 cm^{-1}, respectively. For liquid *n*-alkanes, these frequencies are significantly higher, near 2928 and 2856 cm^{-1}.

In the present study we have also used these bands to monitor chain packing in the gel. The frequencies of the d^- and d^+ bands for a polymethylene crystal consisting of all-*trans* chains depend on packing geometry and density, which in turn depend on temperature (MacPhail et al., 1984). Although changes in conformational disorder and crystal packing produce comparable frequency shifts, the two effects can nevertheless be distinguished. For phospholipid dispersions, the shifts arise from changes in packing if the frequencies of the d^- and d^+ bands are below 2918.8 and 2850.2 cm^{-1}, respectively. Conformational changes are indicated if the d^-- and d^+-band frequencies exceed these values by more than a few tenths of a wave number. A problem in measuring these bands stems from their high intensities relative to those of other bands that we wish to monitor simultaneously. We have therefore tended to employ the symmetric rather than the antisymmetric C—H stretching band, because its intrinsic intensity is substantially less.

Methylene scissors bands

The scissors band was most often used to monitor phase and phase changes in the crystalline state because it is uniquely sensitive to interchain interaction (Snyder, 1960, 1961; Snyder et al., 1995; Mendelsohn et al., 1995). The scissors band has two components for orthorhombic-subcell chain packing. The high-frequency band (1470-1474 cm^{-1}) is designated the *a* component and the low-frequency band (1460-1468 cm^{-1}) the *b* component. The prefixes (*a* and *b*) refer to the axes of the subcell, indicating the direction of the IR transition moment (Snyder, 1961).

The *b* component is significantly more sensitive to structural change than the *a* component. The difference is due to the fact that two kinds of frequency shift are involved, both originating from changes in lateral density. With increasing temperature, the frequencies of the component bands shift upward by the same amount. At the same time, there is a decrease in band splitting. When the two shifts are summed, the result is that the net shift (upward plus downward) of the *a*-component shifts is less than the shift (both upward) for the *b*-component.

LOW-TEMPERATURE ORDERED ORTHORHOMBIC PHASE (G_o)

Identification of G_o at −19°C

The gel-state dispersions of $diC_{18}PC$, $diC_{20}PC$, $diC_{22}PC$, and $diC_{24}PC$ at −20°C can all exist in the ordered orthorhombic G_o phase. The stability of the G_o phase increases markedly with chain length. Depending on (unknown) factors associated with preparation and thermal history of the dispersion, the $diC_{18}PC$ gel at −20°C can be in either phase, unlike $diC_{22}PC$ and $diC_{24}PC$, which were found only as G_o at −19°C.

The G_o and G_d phases can be distinguished from the frequencies and shapes of their scissors bands (Mendelsohn et al., 1995). The bands for these two phases are shown in Fig. 2 for $diC_{18}PC$ at −18°C. The band parameters associated with them, which are discussed below, are listed in Table 2.

The scissors bands of the PCs in the G_o phase at −20°C and the orthorhombic *n*-alkanes near room temperature are quite similar, indicating similar chain packing. This is also indicated by the x-ray measurements of Sun et al. (1996), who found the *a* and *b* dimensions of the unit subcell for $diC_{24}PC$ at 25°C to be, respectively, 7.45 and 4.97 Å, nearly identical to the values 7.47 and 4.97 Å observed for orthorhombic $n\text{-}C_{21}H_{44}$ at 25°C (Small, 1986).

The setting angle θ (the angle between the chain direction and the *a* axis) can be obtained from the intensity ratio (I_a/I_b) of the scissors-band components. The two quantities are related (Snyder, 1961) by

$$\cot\theta = (I_a/I_b)^{1/2}. \quad (1)$$

Using $I_a/I_b = 0.86 \pm 0.12$ from Table 2, we estimate for $diC_{18}PC$ at −19°C a value for θ of ~47 ± 2°, the error coming from the uncertainty in the intensity ratio. For comparison, θ for orthorhombic $n\text{-}C_{23}H_{48}$ at room temperature is estimated from x-ray diffraction measurements to be 42 ± 5° (Smith, 1953).

Temperature dependence of G_o

The scissors bands associated with the G_o phase are shown in Fig. 3 at selected temperatures. Fig. 4 shows their frequencies plotted as a function of temperature.

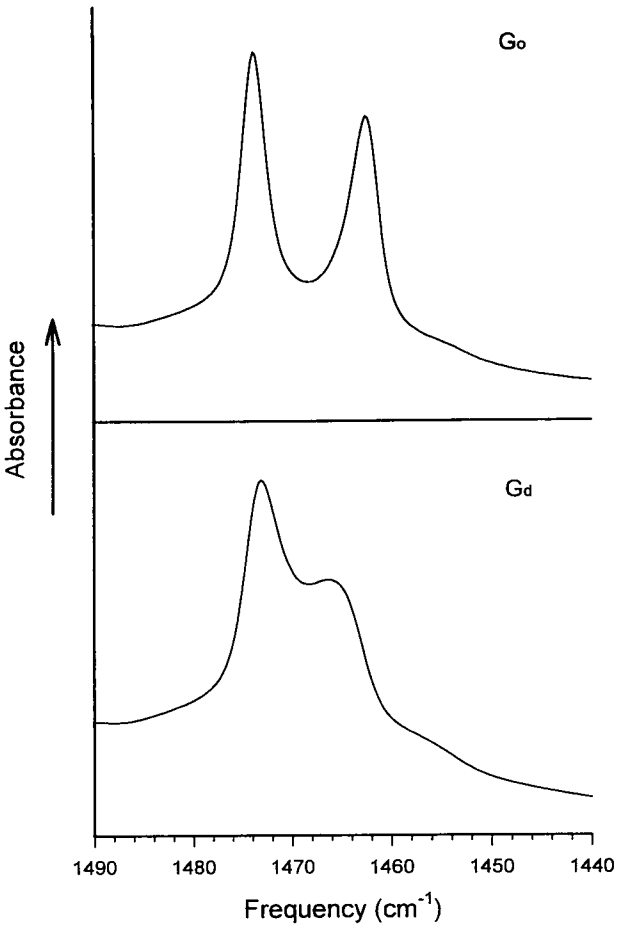

FIGURE 2 IR scissors bands for the low-temperature ordered orthorhombic (G_o) and the ordinary orthorhombic (G_d) phases of $diC_{18}PC$ at −18°C.

As the $diC_{22}PC$ and $diC_{24}PC$ gels are warmed from −20°C, the G_o phases persist virtually unchanged until, at some fairly well-defined temperature, they begin to convert to G_d. Warming the G_o-phase gels results in lateral expansion and a consequent weakening of interchain vibrational coupling. For $diC_{24}PC$ this is manifest in a gradual, nearly linear decrease in the scissors-band splitting that continues to the onset of the G_o-to-G_d transition. The expansion is not accompanied by a significant change in the chain-packing geometry because the setting angle remains nearly constant. From −19 to 32°C the intensity ratio I_a/I_b changes by less than 10%, which corresponds to a setting-angle change of less than 2°.

TABLE 2 Scissors-band parameters measured for the G_o and G_d phases of $diC_{18}PC$ at −19°C

Parameter*	Phase at −19°C	
	G_o	G_d
ν_a#	1473.8	1473.1
ν_b	1462.3	1464.4
$\Delta\nu$	11.5	8.7
$\Delta\nu_{1/2,a}$§	3.3	5.1
$\Delta\nu_{1/2,b}$	4.7	9.9
I_a/I_b¶	0.86	1.37
A_a/A_b‖	1.20	1.87
θ**	47.2	40.5

*Subscripts a and b refer to the *a* and *b* components.
#Frequencies in cm^{-1}.
§Full width at half maximum in cm^{-1}.
¶Integrated intensity ratio (est error: ±0.12).
‖Peak-height ratio.
**Setting angle in degrees (est error: ±2°).

We used the temperature coefficients of the scissors-band frequencies (Table 3) to estimate relative stabilities, with smaller values implying greater stability. By this measure, the stabilities of the G_o phases of $diC_{22}PC$ and $diC_{24}PC$ at −19°C are comparable. However, both are more stable than orthorhombic n-C_{21}, an n-alkane of comparable length. The room-temperature coefficients for n-C_{21} are approximately two to three times larger than those for the gels.

The conformational order of the acyl chains in the G_o phase is very high, comparable with that of the orthorhombic n-alkanes at room temperature (Maroncelli et al., 1985), as might be expected in view of the structural similarities between the bilayer and the orthorhombic n-alkanes.

G_o-TO-G_d TRANSITION: ONSET AND COMPLETION TEMPERATURES

Determination

By IR spectroscopy

Onset and completion temperatures for the G_o-to-G_d phase transition T_b (b = begin) and T_e (e = end) were obtained from the breaks observed in the temperature plots of various band parameters. Inasmuch as phase transitions affect, more or less, all aspects of the structure and dynamics of a crystal, transition temperatures would be expected to be essentially independent of the band or the band parameters chosen. In general, this is what we observe. Slightly different temperatures might result, however, if the phase transition occurred in stages, in which case the maximum response of different band parameters might occur at slightly different temperatures.

From wagging-band intensities. Accurate measurements are difficult because the intensities of these band are low and neighboring bands tend to overlap. The bands that we measured were near 1310 and 1200 cm^{-1}, being farthest removed from the intense P—O stretching band near 1230 cm^{-1} (Fig. 1).

Plots of wagging-band intensity versus temperature show breaks from which T_b and T_e can be determined. As the chains become shorter, the breaks become increasingly diffuse. Fig. 5 shows representative plots: transition temperatures are listed in Table 4.

From C—H stretching-band frequencies. The breaks in the temperature–frequency plots for these bands (Fig. 6) are associated with T_b and T_e. These are fairly well defined for $diC_{22}PC$ and $diC_{24}PC$. The derived transition temperatures are listed in Table 4.

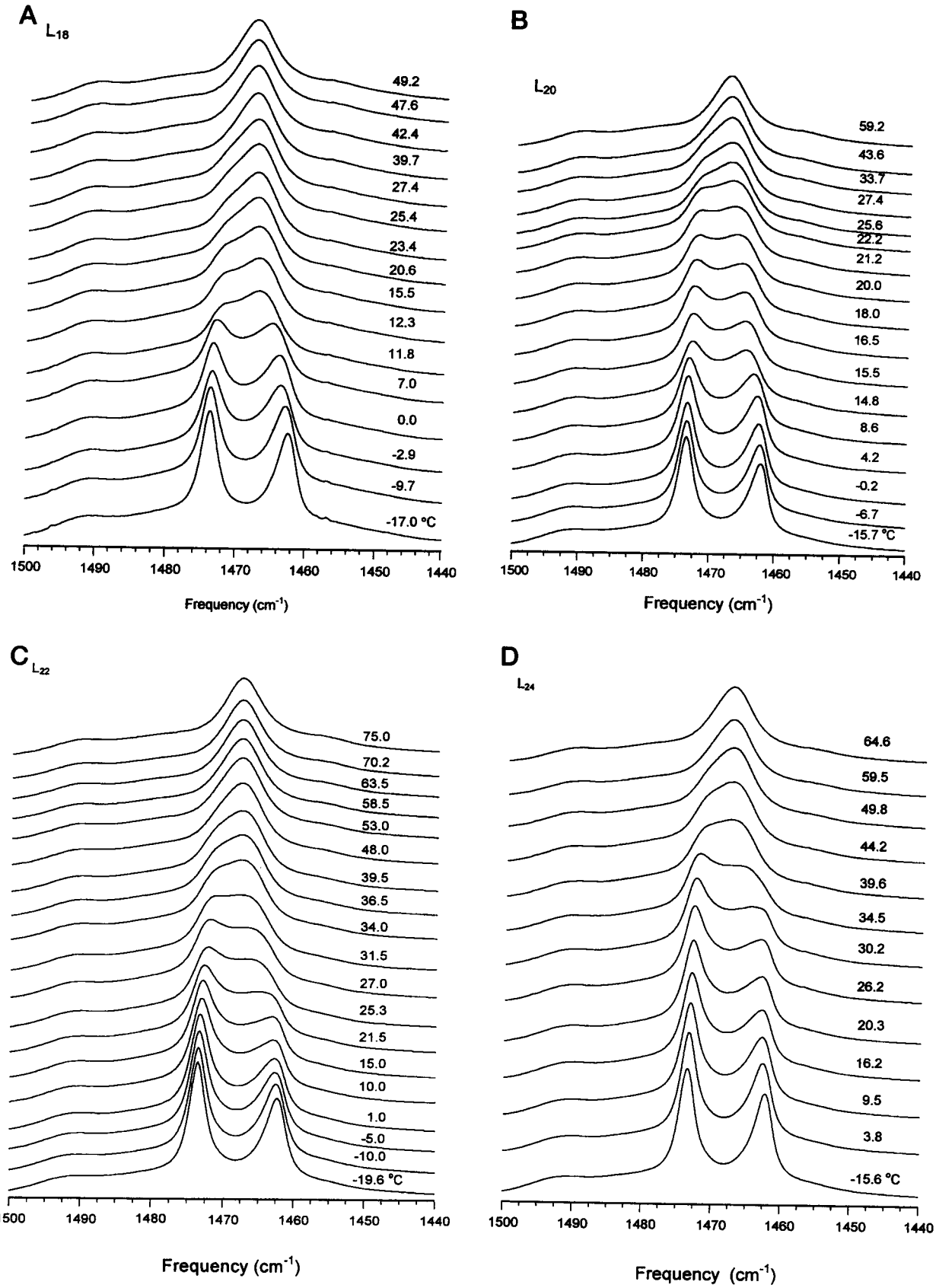

FIGURE 3 Stacked IR absorbance spectra in the scissors-band region for fully hydrated dispersions of diC_nPC at increasing temperatures, which are indicated for each spectrum. At the lowest temperature the gel is in the G_o phase. (*A*) $n = 18$, (*B*) $n = 20$, (*C*) $n = 22$, (*D*) $n = 24$. (In this figure and those that follow, the phospholipids, diC_nPC, are designated *Ln*.)

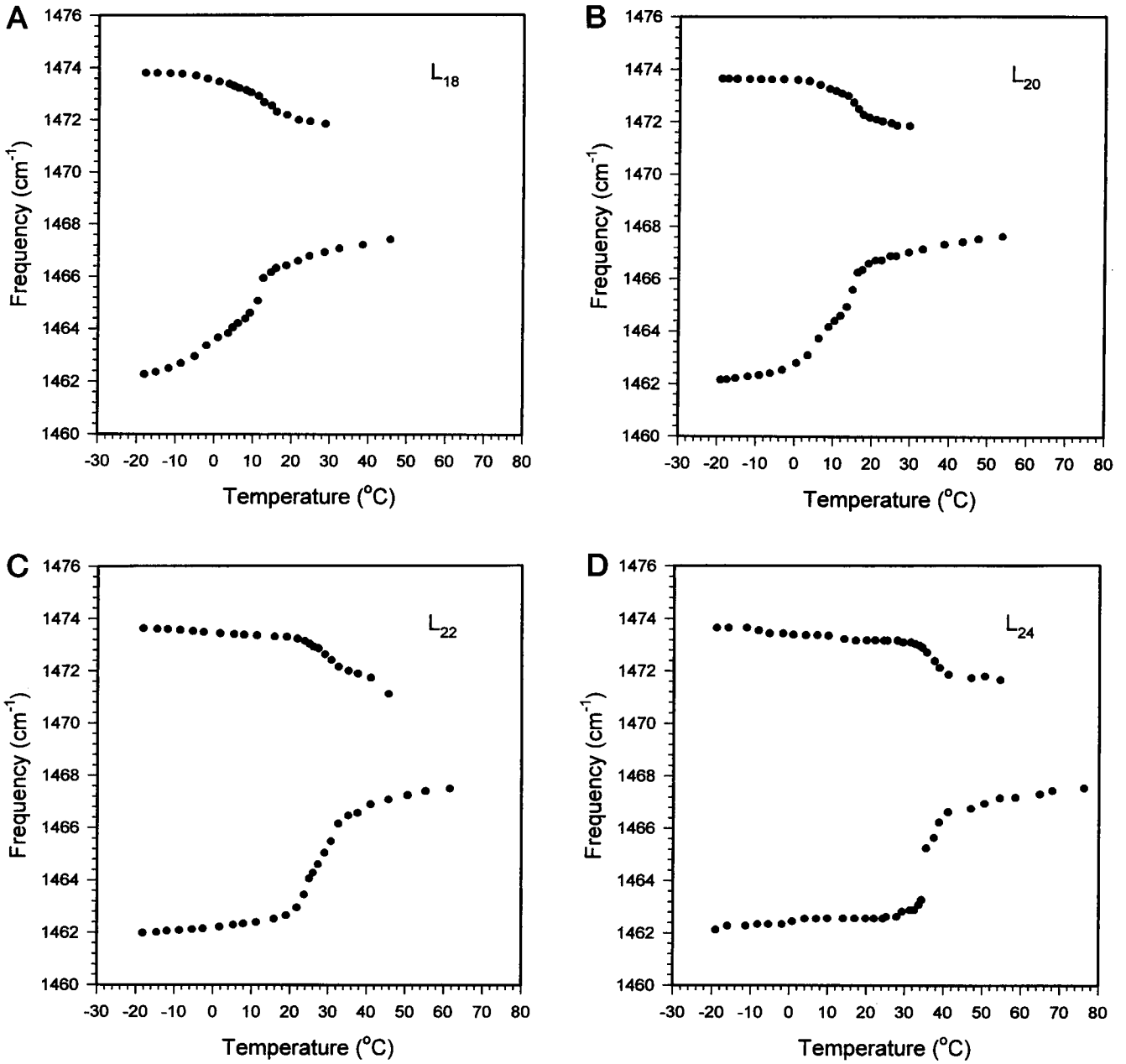

FIGURE 4 Frequencies of the scissors bands for fully hydrated dispersions of diC_nPC plotted as a function of increasing temperature. At the lowest temperature the gels are in the G_o phase. (*A*) $n = 18$, (*B*) $n = 20$, (*C*) $n = 22$, (*D*) $n = 24$.

From the scissors-band frequencies. The temperature–frequency plots (Fig. 4) for the *a*- and *b*-component bands give slightly different values. The *b*-component value is probably more accurate, because this band is more sensitive to structural change. The temperature at which the plots for $diC_{22}PC$ and $diC_{24}PC$ begin to be nonlinear is taken as T_b. On further warming, linearity resumes, and then a second break begins. The value of T_e is assumed to be the temperature at which linearity again resumes. The relation between the transition temperatures and the breaks is illustrated in Fig. 7.

The breaks for $diC_{18}PC$ and $diC_{20}PC$ are more diffuse, and only T_e can be estimated with any accuracy. Its values are in line with those derived from the wagging and C—H stretching bands.

The $diC_{18}PC$ gel can exist in either the G_o or the G_d phase, which allows T_e to be determined by comparison of the temperature–frequency plots for the two phases. With increasing temperature, the G_o and G_d plots (Fig. 8) approach each other and begin to overlap near 13°C. This temperature must correspond to T_e, the temperature at which the G_o phase has been entirely converted to G_d. Its value

TABLE 3 Temperature coefficients of the scissors-band frequencies

	n	Temperature range (°C)	Component	$\partial\nu(\delta)/\partial T$ $(\times 10)^{-2}(cm^{-1}/°)$	Ratio b/a*
DiC_nPC					
G_d phase					
	16	−20 to −5	*a*	−2.1	−1.5
			b	3.2	
	18	−20 to 25	*a*	−4.3	−1.6
			b	7.0	
G_o phase					
	22	−20 to 15	*a*	−0.9	−1.2
			b	1.1	
	24	−20 to 5	*a*	−1.0	−1.5
			b	1.5	
G_d + (G_h) phase					
	18#	40 to 52		1.5	
	18	30 to 45		2.7	
	20	20 to 40		2.8	
	24	40 to 55		4.1	
n-Alkane					
Ortho					
	21	25 to 31	*a*	−3.0	
			b	3.0	

*Ratio $b/a = \partial\nu(\delta_b)/\partial\nu(\delta_a)$.
#Sample in the G_d phase at −19°C.

agrees well with the 12°C determined above from the frequency–temperature plot.

By calorimetry

The DSC scans for $diC_{22}PC$ and $diC_{24}PC$ displayed in Fig. 9 show two (overlapping) endotherms near the expected

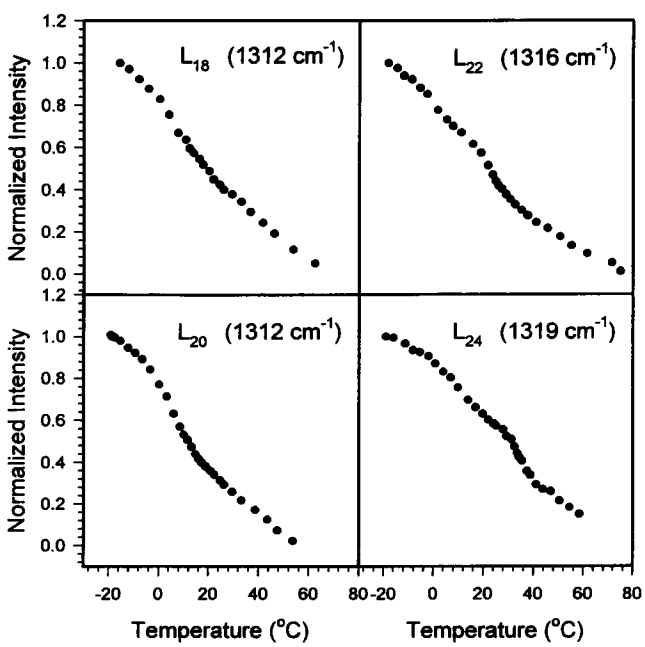

FIGURE 5 Integrated IR intensities of selected wagging bands for diC_nPC (n = 18, 20, 22, 24) plotted against temperature. The inflections are associated with the G_o-to-G_d transition, except for n = 24, in which case there is an "extra" inflection associated with a transition to the G_h phase (see text).

G_o-to-G_d transition temperature. The lower-temperature peak, which is much more prominent, yields values for T_b and T_e near the spectroscopic ones (Table 4 and Fig. 7). Total enthalpies (sum of the two components) are substantial, 1.2 and 3.0 kcal/mol, respectively, for $diC_{22}PC$ and $diC_{24}PC$. The higher-temperature component may be, at least for $diC_{24}PC$, associated with the G_d-to-G_h phase transition discussed below.

DSC endotherms are found for the $diC_{18}PC$ and $diC_{20}PC$ gels (Fig. 9) that have enthalpies of 0.2 and 0.4 kcal/mol, respectively, in line with the trend (smaller values for shorter chains) expected for the G_d-to-G_o transition. However, the transition temperatures are substantially higher than those estimated from IR spectra, possibly because of a shift from nonequilibrium effects of the type reported by Sun et al. (1966) for $diC_{24}PC$. On the other hand, these endotherms may be associated with a different kind of transition, perhaps one involving a subgel phase.

Dependence on chain length

With increasing acyl chain length the G_o-to-G_d transition occurs at a higher temperature and becomes sharper. The shifts are, however, not uniform with chain length (Fig. 4). This is clearly evident in the band-splitting-versus-temperature plots in Fig. 10. The four curves, all sigmoidal, divide into two pairs: n = 18, 20 and n = 22, 24.

The plots of T_b and T_e against chain length shown in Fig. 11 are based on spectroscopic averages and DSC estimates (Table 4). The temperature separations among T_b, T_e, and T_m are roughly constant, that is, they are approximately independent of chain length: T_e is consistently ~40°C below T_m and T_b is ~11°C below T_e.

TABLE 4 Measured onset (T_b) and completion (T_e) temperatures and enthalpies for the G_o-to-G_d phase transition; temperature (T_h') at which G_d is completely converted to G_h

	Transition temperatures						
	Marker used						
			ν (δ)				
n	I (W)	$\nu(d^+)$	a	b	Average (IR)*	DSC*	Enthalpy (ΔH)#
18							0.2
T_b§ =						(10)¶	
T_e =	12	13	11	12	12	(20)¶	
T_h' =			30				
20							0.4
T_b =	3	3	7	5	4	(15)¶	
T_e =	17	17	18	17	17	(35)¶	
T_h' =			32				
22							1.2
T_b =	21		21	22	21	18	
T_e =	31		33	32	32	30	
T_h' =			43				
24							3.0
T_b =	32	31	31	34	32	30	
T_e =	41	40	43	40	41	42	
T_h' =			54				

*Estimated error ±2°.
#kcal/mol.
§Temperatures in °C.
¶Probably not associated with the G_o-to-G_d transition.

USUAL ORTHORHOMBIC PHASE (G_d)

Structure of the G_d phase

The G_d and G_o phases are much alike. Their acyl chains are fully extended and pack in an orthorhombic subcell. Similar chain packing is indicated by the scissors-band splitting, ~9.0 cm^{-1} for G_d and ~11.4 cm^{-1} for G_o near −20°C, and

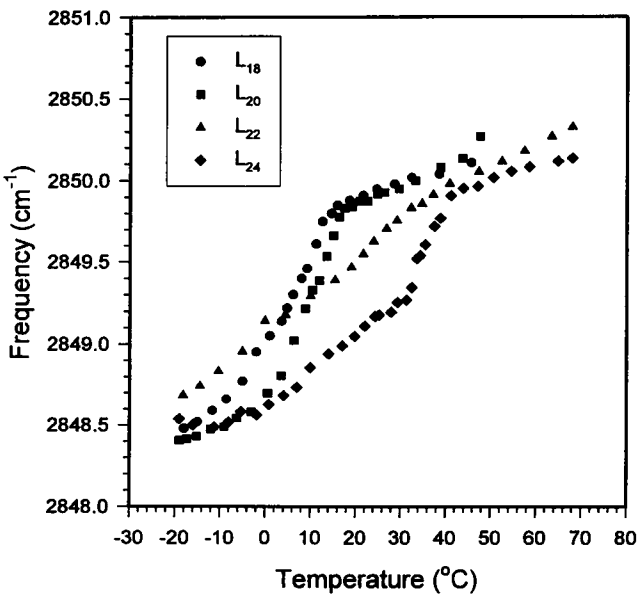

FIGURE 6 Frequencies of the symmetric C—H stretching band for fully hydrated dispersions of diC_nPC (n = 18, 20, 22, 24) plotted as a function of increasing temperature.

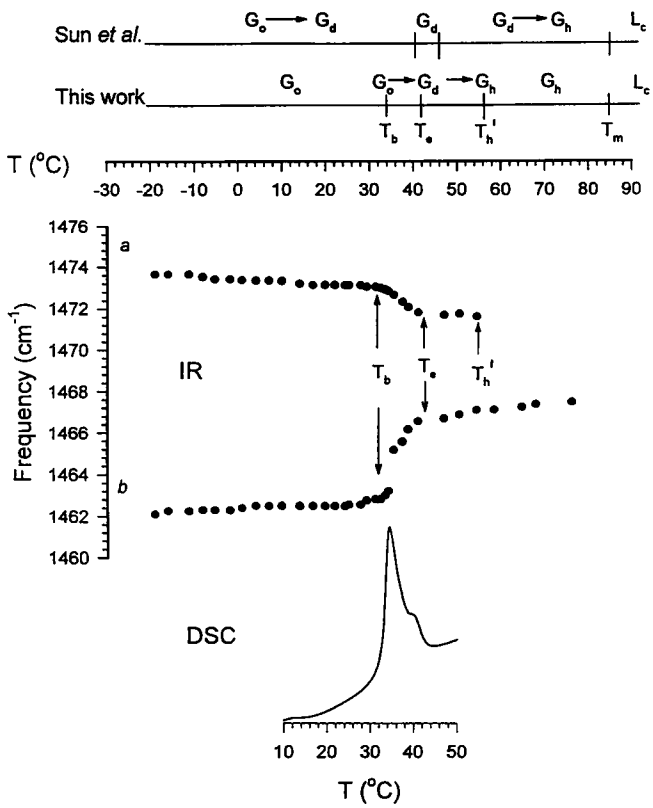

FIGURE 7 Summary of phase behavior for $diC_{24}PC$ in its gel state as determined by x-ray diffraction by Sun et al. (1996) and by IR spectroscopy in the present study.

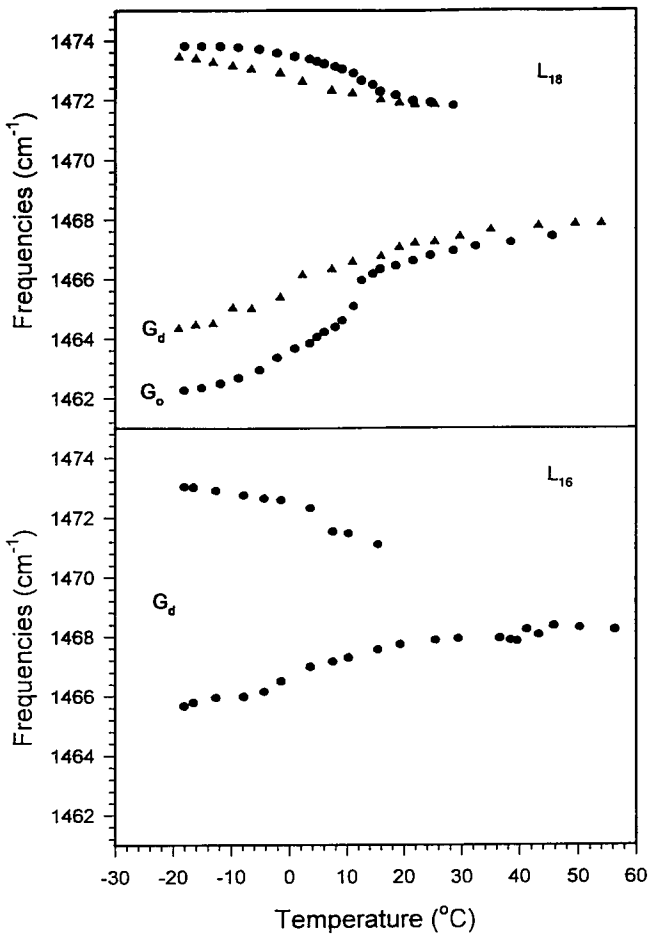

FIGURE 8 Scissors-band frequencies plotted as a function of increasing temperature: (*top*) for $diC_{18}PC$ initially (at −19°C) in the G_o phase and also initially in the G_d phase and (*bottom*) for $diC_{16}PC$ initially in the G_d phase.

also by the setting angle, estimated from Eq. 1 to be $40._5 \pm 2°$ for G_d and $47 \pm 2°$ for G_o.

There are, however, major differences in chain tilt and chain-packing order. The x-ray diffraction measurements by Sun et al. (1996) indicate no appreciable tilting for G_o, in keeping with our spectroscopic evidence that this phase and the orthorhombic phase of the *n*-alkanes are essentially the same. For $diC_{16}PC$ at room temperature the G_d chain tilt is near 32°, increasing a few degrees for longer chains (Tristram-Nagle et al., 1993). For example, Sun et al. (1996) estimated a 34° tilt for the G_d phase of $diC_{24}PC$.

The chain packing in G_d appears to be more disordered than in G_o. This follows from the observation that the widths of the scissors bands are greater for G_d than for G_o. The difference is more evident in the *b* component, as may be seen in Fig. 2 for $diC_{18}PC$ at −19°C. (The bands in this figure are representative of all long-chain PCs in the G_d phase.) The width difference between the two phases is maintained to temperatures as low as −90°C (Cameron et al., 1981) and therefore cannot be attributed to dynamic effects. Conformational disorder can also be ruled out, because its presence does not broaden the scissors bands in this way.

The greater band widths for the G_d phase are most readily explained as the result of orientational disorder associated with random rotational displacement of the chains about their long axes. Dynamic high-amplitude libration occurs in the gel at temperatures approaching T_m. At low temperatures the orientational disorder might involve "frozen-in" chain twisting. Disorder of this type will lead to band broadening by perturbing interchain vibrational coupling (Snyder, 1961), thus producing a distribution of scissors-band frequencies. The disorder may also involve some degree of nonregistering among the methylenes; that is, because the chains are tilted, the planes of the methylenes in neighboring chains, although they are parallel, may be slightly offset.

This disorder is expressible as a distribution of setting angles. We have estimated the root-mean-square (rms) deviation of the setting-angle displacements for the G_d phase of $diC_{18}PC$ from the band broadening. The contribution to the broadening from orientational disorder is taken to be the difference between the width observed for the G_d phase and that for an ordered reference system. Two reference systems were used: the G_o phase of $DiC_{18}PC$ and the orthorhombic phase of n-C_{21}. Only the *b*-component band is considered because its broadening is much larger than for the *a* component. The *b*-component broadening is estimated to be 5.2 cm^{-1} when it is based on the G_o phase (Table 2). It is 6.1 cm^{-1} when based on n-C_{21}, whose room-temperature width is 3.8 cm^{-1}. (The widths are expressed as full widths at half-maximum.)

The spread in the distribution of setting angles can be estimated from the dependence of the frequency of the *b*-component band on the setting angle. The latter can be determined from the changes in the frequency of the *b* component (2.1 cm^{-1}) and in the setting angle (6.7°) in going from the G_o phase at −20°C to the G_d phase at the same temperature. Combining the various quantities leads to a rms deviation in θ of 8.3° or 9.7°, depending on whether the broadening is based on the G_o gel or on orthorhombic n-C_{21}.

The setting-angle deviation for the G_o phase for $diC_{18}PC$ can also be estimated. For this case we used orthorhombic n-C_{21} as the reference. A value of ~1.4° was found.

One final aspect of this phase, which is of interest because of its relevance to the characterization of the gel state of phospholipids by IR spectroscopy, concerns the difference in the sensitivities of the *a*- and *b*-component frequencies to changes in the orthorhombic subcell. As noted above, this difference is responsible for the component bands' behaving differently in going from G_o to G_d. We will use the ratio of their broadening as a measure of the relative sensitivity of the *a*- and *b*-component frequencies to structure change. This ratio (R_W) has a value of 2.9.

A similar measure of relative sensitivity can be derived from the dependence of the frequencies of the *a*- and *b*-component bands on acyl chain length. This dependence is

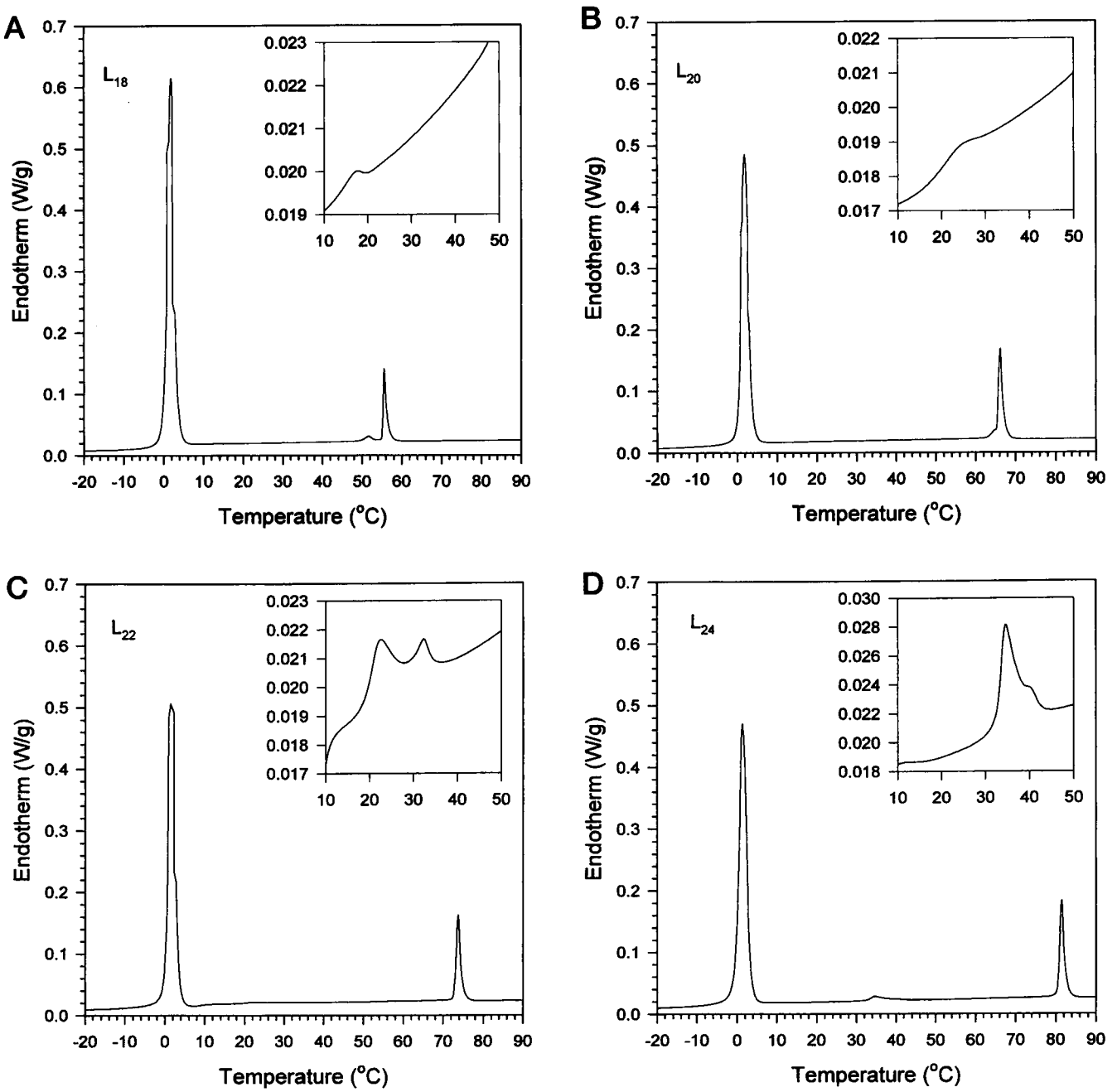

FIGURE 9 DSC scans of fully hydrated dispersions of diC_nPC. Units are watts/gram for a scan rate of 25°C/h: (*A*) $n = 18$, (*B*) $n = 20$, (*C*) $n = 22$, (*D*) $n = 24$.

shown in Fig. 12 for a series of diC_nPC (n = 12–24) gels at low temperature. The *a*-component frequency increases with chain length at a much slower rate than the frequency of the *b* component decreases. The magnitude of the ratio (R_1) of the slopes of the *a* and *b* curves is a measure of relative sensitivity to structural change. The value of R_1 (*b* to *a*) is 1.8 at $n = 13$ and is 3.3 at $n = 20$, to be compared with the value of 2.9 found above for R_W. (We note from Fig. 12 that the splitting of the scissors band increases smoothly from ~8 to ~12 cm^{-1} with increasing chain length. This trend probably reflects a reduction in the steric constraints on chain packing imposed by the headgroup.)

Another, more direct estimate of the relative sensitivities comes from the frequency shifts that the *a*- and *b*-component bands undergo as a result of the G_o-to-G_d transition. In this case the ratio (R_2) of interest is that of the shifts (*b* to *a*). Its value was estimated for $diC_{24}PC$ at the mid-temperature (38°C) of the transition (Fig. 4); the *a* component shifts

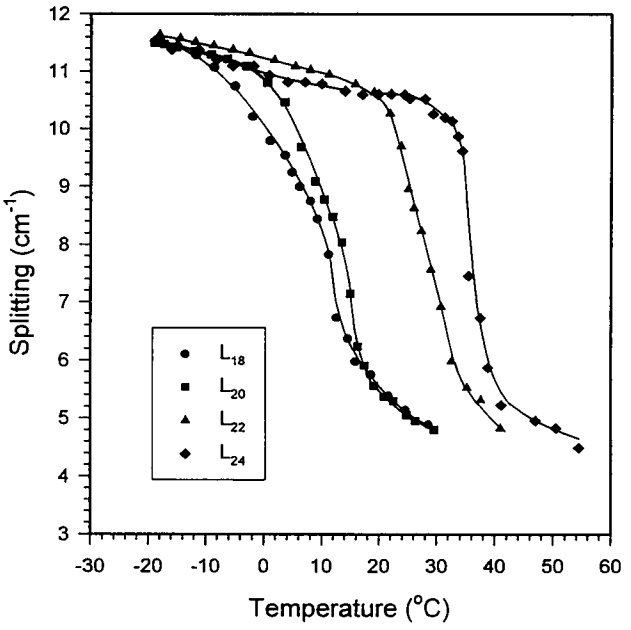

FIGURE 10 Splitting of the methylene scissors bands for fully hydrated dispersions of diC_nPC (n = 18, 20, 22, 24) plotted as a function of increasing temperature. At −19°C the gels are in the G_o phase.

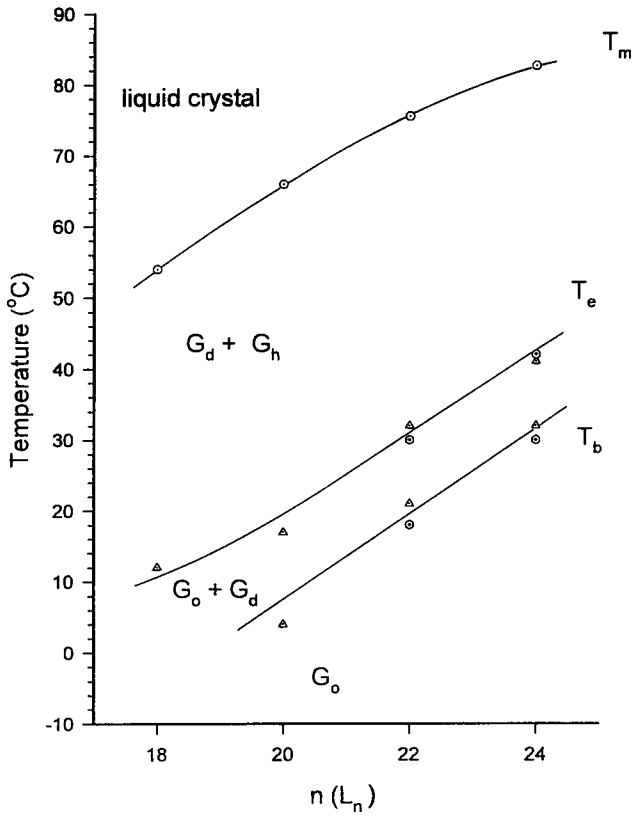

FIGURE 11 Observed onset (T_b) and completion (T_e) temperatures for the G_o-to-G_d transition as a function of chain length: △, spectroscopic averages; ⊙, DSC estimates. The main transition temperature (T_m) is also included.

downward by 1.25 cm^{-1} and the b component upward by 3.90 cm^{-1}. Thus, R_2 is 3.1, very close to the value of 2.9 obtained for R_W from band broadening.

We conclude that the b component is close to three times more sensitive than the a component.

Temperature dependence of the G_d phase

The temperature coefficients of the scissors-band frequency indicate that the G_d phase is thermally less stable than G_o. Specifically, in the temperature region from −20 to −5°C or higher, the coefficients for G_d diC_{16}PC and diC_{18}PC are larger by at least a factor of 2 than those for G_o diC_{22}PC and diC_{24}PC (Table 3). The difference is not due to chain-length differences because the temperature coefficient for diC_{16}PC is larger than for diC_{18}PC and, likewise, that for diC_{22}PC is larger than for diC_{24}PC.

The temperature coefficients for the a component are smaller than for the b component for both G_o and G_d (Table 3). This finding is in line with the known greater sensitivity of the b component to structural change. The ratio of the coefficients (b to a) is ~1.5, approximately half of that found for a change in packing.

TRANSITION FROM G_d TO A PHASE WITH HEXAGONAL CHAIN PACKING

As the temperature of the gel is increased from T_e to T_m a new phase (G_h) appears whose scissors-band frequency (1467.5 cm^{-1}) and contour (featureless) indicate hexagonal or hexagonal-like chain packing of the type associated with orientational disorder. With chains that are all-*trans* this phase seems closely related to the ripple phase and, in fact, may be the ripple phase.

At a temperature just above the G_o-to-G_d transition the G_d and G_h phases coexist, as evidenced by the fact that bands from both phases appear in the IR spectrum. As the temperature increases above T_e, a conversion of G_d to G_h occurs because the intensity of the a-component band of G_d decreases while the frequency and breadth of the band remain nearly unchanged. The conversion to G_h is complete at a temperature designated T_h', which is well below T_m. Values of T_h' were determined from the frequency–temperature plots (Fig. 7) for gels initially in the G_o phase at −20°C. T_h' is estimated to be 30, 32, 43, and 54°C for n = 18, 20, 22, 24, respectively (Table 4). Measurements of n = 16 and n = 18 gels that were in the G_d phase at −20°C gave values for T_h' near 18 and 30°C, respectively.

The existence of a G_d-to-G_h transition is supported by the presence of a third inflection in the wag intensity–temperature plot for diC_{24}PC, which is more clearly discernible in the full-scale plot than in the reduced plot shown in Fig. 5. The value of T_h' thus obtained is 50°C, reasonably close to the 54°C obtained above from the a component of the scissors band.

As judged by the scissors frequency, the G_h phases for the gels n_{even} = 16–24 are virtually identical. At temperatures

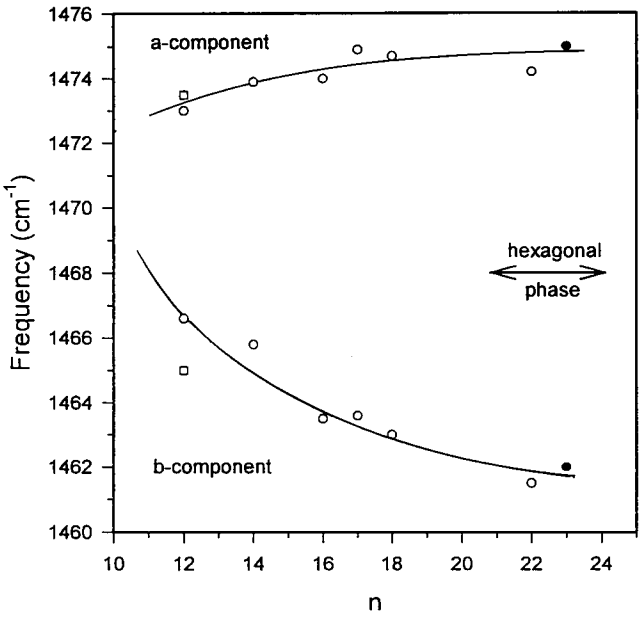

FIGURE 12 Frequencies of the *a* and *b* components of the scissors band plotted against chain length for diC$_n$PC dispersions in the gel state at temperatures below −90°C: ○, ●, respectively, the lipids and C_{23} at −180°C; □, the lipids at −100°C. The frequencies for the lipids are from Cameron et al. (1981); those for the *n*-alkane, *n*-C_{23}, are from our own measurements.)

just above T_h' the scissors frequencies all fall between 1467.0 and 1467.6 cm^{-1}, and at higher temperatures (5–15°C below T_m) they are between 1467.6 and 1468.0 cm^{-1}.

Chain interaction in the G_h phase weakens as temperature increases above T_h. This is indicated by a narrowing of the scissors band: for diC$_{18}$PC, for example, the width of this band goes from 6.1 cm^{-1} at 44°C to 5.5 cm^{-1} at 54°C. Similar narrowing for diC$_{16}$PC was reported by Cameron et al. (1980).

As T_m is crossed, the chains become conformationally disordered. The result is an increase in the scissors-band width of ~1 cm^{-1}, a frequency decrease of ~0.5 cm^{-1}, and a pronounced increase in asymmetry in the form of relative intensity enhancement on the low-frequency side.

DISCUSSION AND SUMMARY

G_o phase

Gel-state fully hydrated dispersions of "long-chain" diacylphosphatidylcholines (diC$_n$PC, n_{even} = 18–24) can exist in a highly ordered orthorhombic phase (G_o) at −19°C. The acyl chains in this phase are all-*trans* and pack in an orthorhombic subcell that is virtually indistinguishable from that found for orthorhombic *n*-alkanes.

The transition temperatures of the G_o phase increase nonuniformly with acyl chain length in a manner indicating that, in terms of stability, diC$_{18}$PC and diC$_{20}$PC can be paired, as, likewise, diC$_{22}$PC and diC$_{24}$PC can be. The G_o phase of diC$_{24}$PC is stable up to ~32°C, but, on warming, the subcell undergoes lateral expansion while the setting angle remains nearly constant.

Comparison of the G_o and G_d phases

The G_o phase is similar to that of G_d, which is the usual phase for gel-state dispersions of "short-chain" PCs (n_{even} < 18). In both G_o and G_d the acyl chains are highly ordered (all-*trans*) and pack in an orthorhombic subcell. The subcell setting angle for G_d is only slightly less than that for G_o, and the thermal stabilities of the two phases are comparable, G_o being somewhat the more stable.

There are, however, major differences in chain tilt and in chain-packing disorder. The x-ray measurements of Sun et al. (1996) of diC$_{24}$PC show the chains in the G_o phase to be nearly perpendicular to the lamellar surface, whereas those in the G_d phase are tilted. IR measurements indicate the chains in the G_d phase are orientationally disordered as if there were a distribution of setting angles.

G_o-to-G_d phase transition

Warming the G_o phase results in a transition to G_d. This transition occurs at higher temperatures and becomes better defined when one goes to longer chains. The onset (T_b) and completion (T_e) temperatures for the G_o-to-G_d transition increase in parallel to the increase in T_m: T_e is ~40°C below T_m, and T_b is ~11°C below T_e.

The DSC derived G_o-to-G_d transition temperatures for diC$_{22}$PC and diC$_{24}$PC are near those determined spectroscopically; the corresponding enthalpies are ~1.2 and ~3.0 kcal/mol, respectively. Endotherms with smaller enthalpies were found for diC$_{18}$PC and diC$_{20}$PC. However, they gave transition temperatures well removed from the spectroscopic values.

Transition from G_d to G_h

At temperatures just above the G_o-to-G_d transition the G_d phase coexists with a high-temperature phase (G_h). The latter exhibits hexagonal-like chain packing that suggests the ripple phase. At a temperature T_h' well below T_m the G_d is completely converted to G_h.

Comparison with x-ray diffraction results

Our IR results and those from x-ray diffraction (Sun et al., 1996) for diC$_{24}$PC are generally in accord. Comparison is straightforward, because each technique provides markers that uniquely identify specific phases. Our study confirms the existence of a new orthorhombic phase (G_o) that has a higher density than the usual orthorhombic phase (G_d). We also find that, with increasing temperature, the G_o phase undergoes a transition to G_d, which in turn converts to G_h.

The few differences between our results and those of Sun et al. (1996) are likely attributable to nonequilibrium effects

that have their origin in sample preparation and processing. A comparison of the phase behavior of the $diC_{24}PC$ gel, as determined by each technique, is shown in Fig. 7. In the lowest-temperature region we observed only the G_o phase, whereas Sun et al. (1996) observed both G_o and G_d. This difference is probably the result of our samples' being cooled to a significantly lower temperature (−20°C) than those in the diffraction study. At a temperature just above the G_o-to-G_d transition we found G_d and G_h to coexist; with warming, we found that G_d converted to G_h, the conversion being complete well below T_m. On the other hand, Sun et al. (1996) found only the G_d phase above the G_o-to-G_d transition; they also found G_d and G_h coexistence and a gradual conversion of G_d to G_h in going to higher temperatures. However, they found coexistence up to T_m.

We thank Professor John Nagle for informative and stimulating discussions and for generously providing us in advance of publication the results of the x-ray studies on the long-chain lecithins carried out at Carnegie Mellon University. We gratefully acknowledge support from the National Institutes of Health (GM-27690 to the University of California at Berkeley and GM-29864 to Rutgers University at Newark).

REFERENCES

Cameron, D. G., H. L. Casal, and H. L. Mantsch. 1980. Characterization of the pretransition in 1,2-dipalmitoyl-*sn*-glycero-3-phosphocholine by Fourier transform infrared spectroscopy. *Biochemistry.* 19:3665–3672.

Cameron, D. G., E. F. Gudgin, and H. H. Mantsch. 1981. Dependence of acyl chain packing of phospholipids on the head group and acyl chain length. *Biochemistry.* 20:4496–4500.

Cevc, G., and D. Marsh. 1987. Phospholipid Bilayer: Physical Principles and Models. John Wiley & Sons, New York.

Lewis, R. N. A. H., N. Mak, and R. N. McElhaney. 1987. Differential scanning calorimetric study of the thermotropic phase behavior of model membranes composed of phosphatidylcholines containing linear saturated fatty acyl chains. *Biochemistry.* 26:6118–6126.

Lewis, R. N. A. H., and R. N. McElhaney. 1991. The mesomorphic phase behavior of lipid bilayers. *In* The Structure of Biological Membranes. P. Yeagle, editor. CRC Press, Boca Raton, FL. Chap. 2.

MacPhail, R. A., H. L. Strauss, R. G. Snyder, and C. A. Elliger. 1984. C—H stretching modes and the structure of *n*-alkyl chains. II. Long, all-*trans* chains. *J. Phys. Chem.* 88:334–341.

Maroncelli, M., H. L. Strauss, and R. G. Snyder. 1985. The distribution of conformational disorder in the high-temperature phases of the crystalline *n*-alkanes. *J. Chem. Phys.* 82:2811–2824.

Mendelsohn, R., G. L. Liang, H. L. Strauss, and R. G. Snyder. 1995. IR spectroscopic determination of gel state miscibility in long-chain phosphatidylcholine mixtures. *Biophys. J.* 69:1987–1998.

Moore, D. J., and R. Mendelsohn. 1994. Adaptation to altered growth temperatures in *Acholeplasma laidlawii*. B: Fourier transform infrared studies of acyl chain conformational order in live cells. *Biochemistry.* 33:4080–4085.

Senak, L., D. Moore, and R. Mendelsohn. 1992. CH_2 wagging progressions as IR probes of slightly disordered phospholipid acyl chain states. *J. Phys. Chem.* 96:2749–2754.

Small, D. M. 1986. Chapter 2. *In* The Physical Chemistry of Lipids. Plenum Publishing Corp., New York.

Smith, A. E. 1953. The crystal structure of the normal paraffin hydrocarbons. *J. Chem. Phys.* 21:2229–2231.

Snyder, R. G. 1960. Vibrational spectra of crystalline *n*-paraffins. Part 1. Methylene rocking and wagging modes. *J. Mol. Spectrosc.* 4:411–433.

Snyder, R. G. 1961. Vibrational spectra of crystalline *n*-paraffins. Part II. Intermolecular effects. *J. Mol. Spectrosc.* 7:116–144.

Snyder, R. G. 1967. A revised assignment of the B_{2g} methylene wagging fundamental of the planar polyethylene chain. *J. Mol. Spectrosc.* 23: 224–228.

Snyder, R. G., M. Maroncelli, H. L. Strauss, and V. M. Hallmark. 1986. Temperature and phase behavior of infrared intensities: the polymethylene chain. *J. Phys. Chem.* 90:5623–5630.

Snyder, R. G., and J. H. Schachtschneider. 1963. Vibrational analysis of the *n*-paraffins. I. *Spectrochim. Acta.* 19:85–116.

Snyder, R. G., H. L. Strauss, and D. A. Cates. 1995. Detection and measurement of microaggregation in binary mixtures of esters and of phospholipid dispersions. *J. Phys. Chem.* 99:8432–8439.

Snyder, R. G., H. L. Strauss, and C. A. Elliger. 1982. C—H stretching modes and the structure of *n*-alkyl chains. I. Long, disordered chains. *J. Phys. Chem.* 86:5145–5150.

Sun, W.-S., S. Tristram-Nagle, R. M. Suter, and J. F. Nagle. 1996. Anomalous phase behavior of long chain saturated lecithin bilayers. *Biochim. Biophys. Acta* 1279:17–24.

Tristram-Nagle, S., R. Zhang, R. M. Suter, C. R. Worthington, W.-J. Sun, and J. F. Nagle. 1993. Measurement of chain tilt angle in fully hydrated bilayers of gel phase lecithins. *J. Biophys.* 64:1097–1109.